International Specialty Conference on Cold-Formed Steel Structures

Wei-Wen Yu International Specialty Conference on Cold-Formed Steel Structures 2018

Nov 7th, 12:00 AM - Nov 8th, 12:00 AM

Experimental Study of Apex Connection Stiffness and Strength of Cold-Formed Steel Double Channel Portal Frames

J. Peng

J. Bendit

H. B. Blum

Wei-Wen Yu International Specialty Conference on Cold-Formed Steel Structures
St. Louis, Missouri, U.S.A., November 7 & 8, 2018

Experimental study of apex connection stiffness and strength of cold-formed steel double channel portal frames

J. Peng[1], J. Bendit[1], H.B. Blum[2]

Abstract

Cold-formed steel portal frames are an increasingly popular structure in the housing and industrial sectors, and are commonly used for garages, sheds, and shelters. Longer span cold-formed steel portal frames are relatively new to the market, and as a result limited design guidance and recommendations exist, including the strength and stiffness of the connections. The apex connection stiffness affects the distribution of internal actions and deflections of a portal frame, and therefore, it is necessary to quantify the apex stiffness for use in design models to accurately determine the frame behavior. An experimental program was carried out on a series of twelve apex connections of portal frames composed of back-to-back lipped channels for the rafters and back-to-back lipped L apex brackets, which were connected by bolts through the webs. The channels had a depth of either 200 or 150 millimeters, and thickness of 1.5, 1.9, or 2.4 millimeters. The apex brackets were 2.4 millimeters thick, and the dimensions varied to match with the connecting rafter sections. The apex connection stiffness and strength were quantified, and the effects of rafter thickness and depth on the connection stiffness and strength were determined. The aim of this work is to quantify the apex connection stiffness of cold-formed steel portal frames composed of back-to-back channels and L-brackets to enable practicing engineers to accurately determine the internal actions and deflections of portal frames.

[1]Research Assistant, School of Civil Engineering, University of Sydney, Sydney, NSW, Australia

[2]Corresponding Author. Associate Lecturer, School of Civil Engineering, University of Sydney, Sydney, NSW, Australia

1 Introduction

Long-span cold-formed steel portal frames are becoming increasingly popular structures, yet limited detailed design guidance and recommendations exist in the literature. Connections are typically formed by bolting plates, or brackets, in between the channel sections. These connections are found to be semi-rigid (Yu et al., 2005). The internal actions and deflections of portal frames are affected by the connection stiffness, yet without known connection stiffness, a connection is usually assumed to be either pinned or rigid. Therefore, incorrect frame behavior can be estimated if correct connection stiffness is not quantified. Internal actions and deflections of a portal frame are typically determined by a second order elastic analysis of a beam finite element model, where the semi-rigidity of the connection can be represented by an in-plane rotational spring.

Previous research has been conducted on apex connections of cold-formed steel portal frames composed of back-to-back channels for the main frame members. Tested apex connections had various apex bracket sizes and thickness, bolt-group sizes, tightness of bolts, and bolts in the bracket web only, or both web and flange (Dubina et al., 2004; Kirk, 1986; Lim and Nethercot, 2004; Zhang et al., 2016). The work presented herein aims to expand the available data on the stiffness and performance of bolted apex connections in cold-formed steel portal frames.

2 Test Setup

A series of twelve tests on the apex connections of cold-formed steel portal frames has been conducted. The rafters consisted of back-to-back lipped channels bolted together through the webs, and the apex brackets consisted of back-to-back lipped L-brackets bolted through the webs. Various channel sizes and thickness were tested, including section depths of 203 mm with a thickness of either 1.5, 1.9, or 2.4 mm, and section depths of 152 mm with a thickness of 1.5, 1.9, or 2.4 mm. There were two apex bracket sizes: one for the 203 mm depth channels, and one for the 152 mm depth channels, both of which were 2.4 mm thick. The nominal channel dimensions for each test are shown in Table 1, and the brackets are shown in Figure 1. Measured dimensions and thicknesses of the channels and brackets are given elsewhere (Bendit, 2017; Peng, 2017).

The apex connection specimens were approximately 2 m long, and are shown in Figure 2. The channel and apex brackets were bolted together with grade 8.8 M14 bolts for the C150 tests, and M16 bolts for the C200 tests. At other locations,

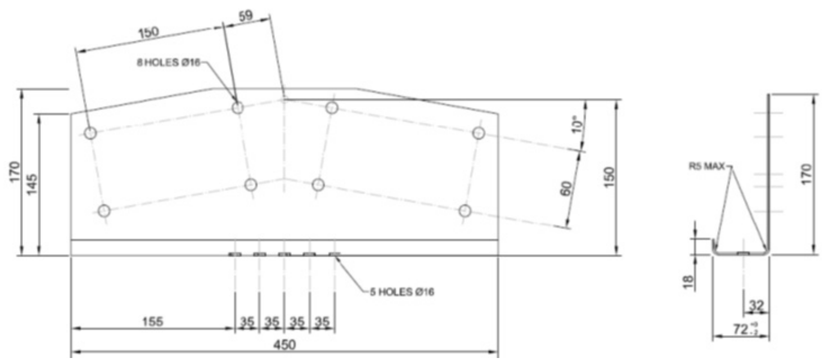

(a)

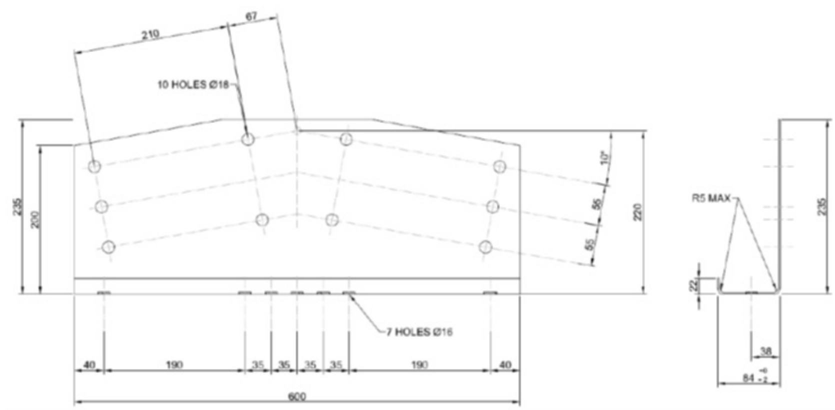

(b)

Figure 1: Apex brackets (a) for C150 rafters and (b) for C200 rafters

Table 1: Nominal dimensions and thickness of connected members in the apex connection tests

Test #	Channel Size	Channel dimensions (mm) web × flange × lip	Channel dimensions (mm) t	Apex bracket Size	Apex bracket t (mm)
1,2	C200-15	203 × 76 × 15.5	1.5	C200	2.4
3,4	C200-19	203 × 76 × 19.0	1.9	C200	2.4
5,6	C200-24	203 × 76 × 21.0	2.4	C200	2.4
7,8	C150-15	152 × 64 × 15.5	1.5	C150	2.4
9,10	C150-19	152 × 64 × 16.5	1.9	C150	2.4
11,12	C150-24	152 × 64 × 18.5	2.4	C150	2.4

the channels were bolted together with grade 4.6 M12 bolts with integrated washers. All bolts were tightened according to the snug tight plus half a turn method, whereby the nut is tightened with the full effort of a person using a standard podger spanner, and then an electric impact wrench is used to turn the nut an additional half turn. The channels and the apex brackets were fabricated using G450 steel, which indicates a nominal minimum yield stress of 450 MPa. Coupon tests from the channels and brackets were conducted according to the Australian Standard (AS 1391, 2007) and it was found that the material had an average Young's Modulus of 206 GPa and an average 0.2% proof stress of 508 MPa. Further details are given elsewhere (Bendit, 2017; Peng, 2017).

The aim of this series of tests was to quantify the in-plane rotational stiffness of the apex connection, which is most influenced by the bending moment. In the apex region of a portal frame with applied gravity loads, the apex is under a constant bending moment. Therefore, symmetric point loads were applied on the rafters (Figures 2 and 3(a)) to produce a constant bending moment in the apex connection. Lateral restraints, consisting of two turnbuckles each, were connected at four locations along the rafters at the locations where purlins would be connected in full frames. Location of the lateral restraints are show in Figure 2 and the turnbuckles are shown in Figure 3(e).

Vertical load was applied by a hydraulic jack which was displacement controlled at a rate of 0.2mm/min. A load spreading beam was used to transfer the applied load onto the rafters at each side of the apex connection through a loading saddle. The saddle transferred the load through a pin in the rafters (Figure 3(b)). Teflon plates were placed between the loading beam and the saddle and a stiffening plate was bolted to the rafters at the location of the loading pin to prevent local failure due to the applied load.

The rafter ends were supported by two half-rounds which were inclined to be perpendicular to the rafters. A teflon plate was placed in-between the bottom of the half-round and its bottom plate, to allow movement as the apex connection pushed outwards during the test. This created a simple support, and therefore prevented the introduction of external compressive forces into the specimens. Rafter boots were bolted onto the rafter ends to increase the torsional rigidity of the specimen ends.

3 Instrumentation

The locations of instrumentation utilized in the experiments are shown in Figure 4. Six linear variable displacement transducers (LVDTs) with 100 mm stroke length were placed at three locations along the apex connection, two each at the left rafter, the bracket center, and at the right rafter, to measure global movements vertically. Measurements were recorded from the attached measuring plates which were located at the centerline of the rafters or at the bottom of the apex bracket. The out-of-plane twist of the specimens could also be determined from these LVDTs, as shown in Figure 5. Three LVDTs with 50 mm stroke length were positioned at the apex bracket to measure out-of-plane displacements. Photographs of these LVDTs are shown in Figure 3(c) and (d) and the locations of their positions are shown in Figure 4(c) and (d).

Eight inclinometers were used to measure the in-plane rotations at four locations along the specimen: the apex bolt group centers and just outside the apex bracket, at each side of the apex connection, as shown in Figure 4. Two inclinometers were attached at each location, one at the front face and the other at the back face. The inclinometers were attached on the rafter longitudinal center-lines.

4 Results

As load was applied causing an opening of the apex connection, the specimen deflected downwards. Eventually, the apex bracket began to buckle in the web, where one side deflected forwards and the other side deflected backwards by a few millimeters. A failed specimen is shown in Figure 6(a) and (b). Load application continued after reaching the ultimate load to capture post-peak behavior. The apex bracket web out-of-plane displacements increased after reading peak load. This produced an eccentricity in the load path of the two rafters, which resulted in a significant reduction in the post-peak connection rotational stiffness. All specimens had similar failure modes. Out-of-plane rotations were measured during the test with the vertical LVDTs, as discussed in Section 3. At peak load, the rotations

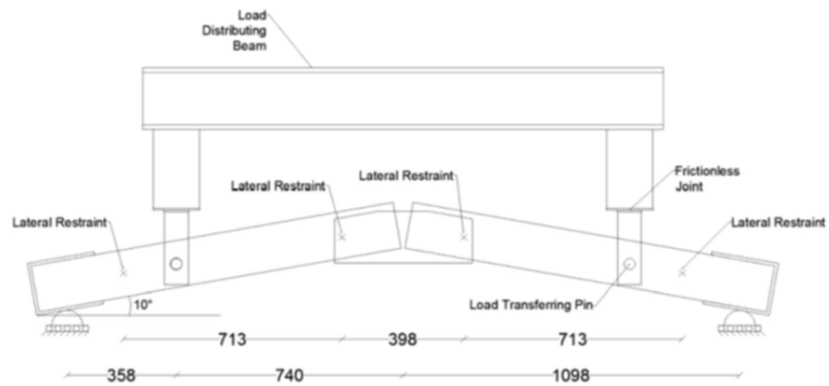

(a)

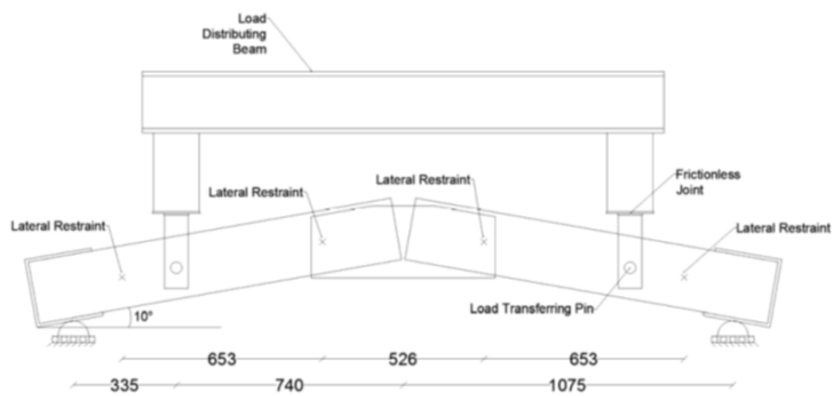

(b)

Figure 2: Test setup showing position of lateral restraints (a) C150 tests, and (b) C200 tests

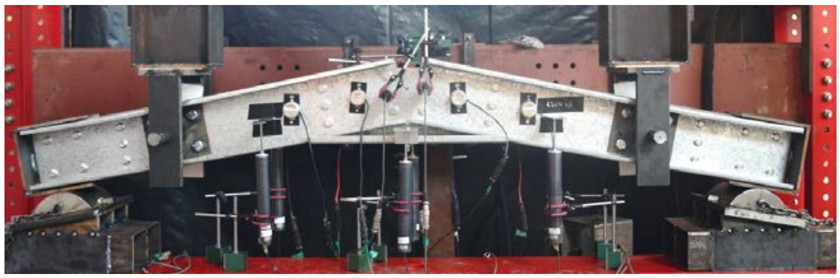

(a)

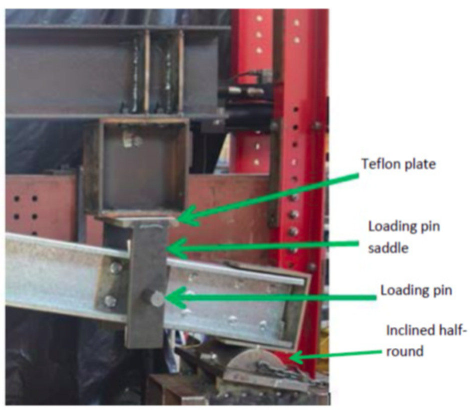

(b)

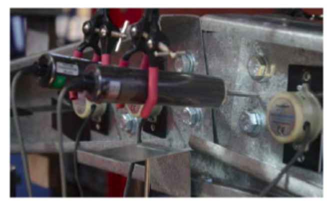

(c)

(d)

(e)

Figure 3: Photos of test setup and instrumentation (a) specimen in test rig, (b) load application details, (c) front transducers, (d) back transducer, and (e) lateral restraints shown on half of the specimen

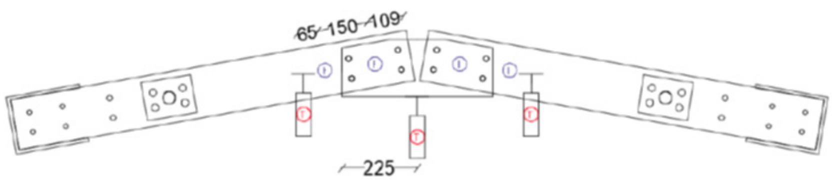

(a)

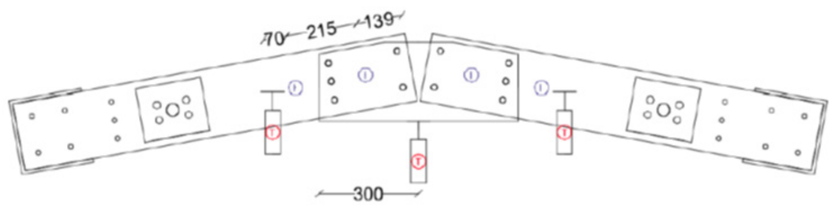

(b)

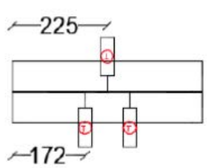

(c)

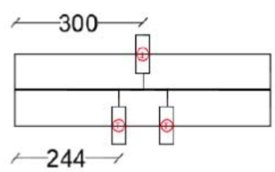

(d)

Figure 4: Position of LVDTs (red T) and inclinometers (blue I) (a) elevation view C150 specimens, (b) elevation view C200 specimens, (c) plan view C150 specimens, and (d) plan view C200 specimens

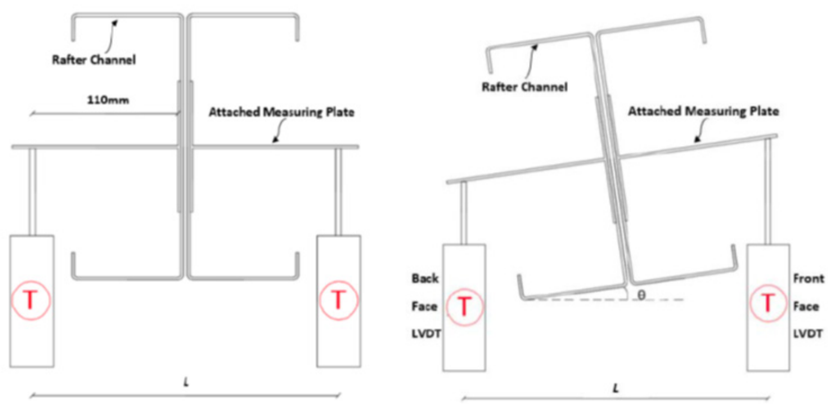

(a)

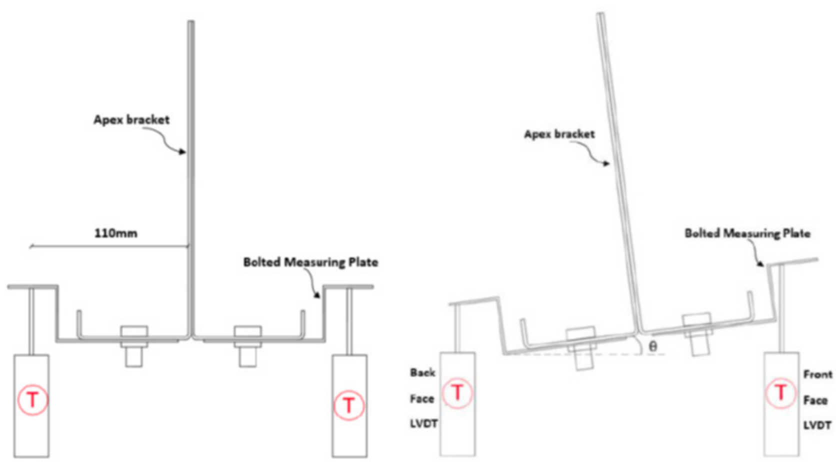

(b)

Figure 5: Vertical LVDTs used for measuring the specimen out-of-plane rotation (a) at the rafters and (b) at the apex bracket

were small but increased during post-peak loading. Full results of the out-of-plane rotations and displacements for each test are given elsewhere (Bendit, 2017; Peng, 2017).

As the connection opened, the top of apex bracket web was under compression. Failure occurred in the apex bracket, as there was no top flange to restrain the top edge of the web from buckling. Additionally, the center of the apex bracket is a weak point in the connection, as the rafters were not connected at this location, thus solely the apex brackets were resisting the applied loads.

Rotations at the center of the apex bolt-groups were measured by four inclinometers, as discussed in Section 3. A single rotation value was obtained by calculating the average of the four inclinometers. The bending moment in the connection was calculated from the applied load using statics. The resulting moment-rotation curves are shown in Figure 7(a) for C150 specimens and 7(b) for C200 specimens. At the start of the test, the specimen was supporting the full weight of the load distributing system, which was 1.67 kN. Therefore, the moment-rotation plots begin at the moment induced in the specimens due to the initial weight of the loading system. The rotations measured at the rafters just outside the apex brackets were larger than those measured at the bolt-group centers, due to bending of the rafter sections. Plots of these rotations are given elsewhere (Bendit, 2017; Peng, 2017).

After removal of the load the specimens were disassembled. Permanent deformations remained in the apex bracket web, as shown in Figures 6(c) and (d). No plastic deformation was evident on the rafters, as shown in Figure 6(e), and no bolt-hole elongation was evident in either the rafters or apex brackets.

The initial linear in-plane rotational stiffness for each test was determined using a linear regression analysis. The upper bounds for the initial linear region was selected as 9 kNm for all C200 specimens, 6 kNm for the C150-15 and C150-19 specimens, and 3.5 kNm for the C150-24 specimens. The initial connection stiffness, $K_{initial}$, for each test along with the ultimate bending moment, M_u, are shown in Table 2. The yield moment capacity, M_y, can be calculated for the apex bracket and rafter sections by $M_y = S \times f_y$, where S is the elastic section modulus of the member under consideration based on the measured geometry, and f_y is the material yield stress determined from the coupon tests. M_y of the apex brackets was calculated as 19.1 kNm and 38.8 kNm for the C150 bracket and the C200 bracket, respectively. M_y of the C150 rafter channels was calculated as 21.4 kNm, 27.0 kNm, and 34.0 kNm for the 1.5 mm, 1.9 mm, and 2.4 mm thick channels, respectively and M_y of the C200 rafter channels was calculated as 35.3 kNm, 45.1 kNm, and 56.9 kNm for the 1.5 mm, 1.9 mm, and 2.4 mm thick channels,

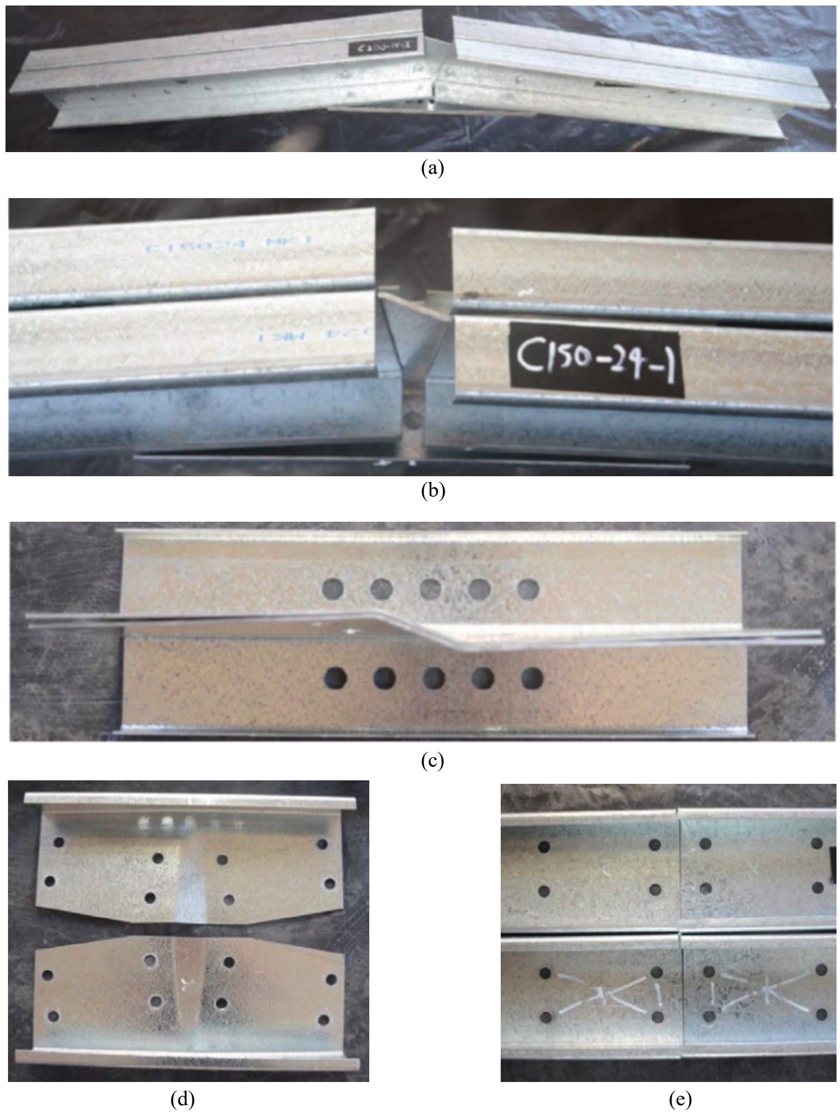

Figure 6: Apex bracket failure (a) full specimen, (b) close up of apex bracket in specimen, (c) apex bracket top view, (d) apex brackets disassembled, and (e) rafter ends connected to bracket, disassembled

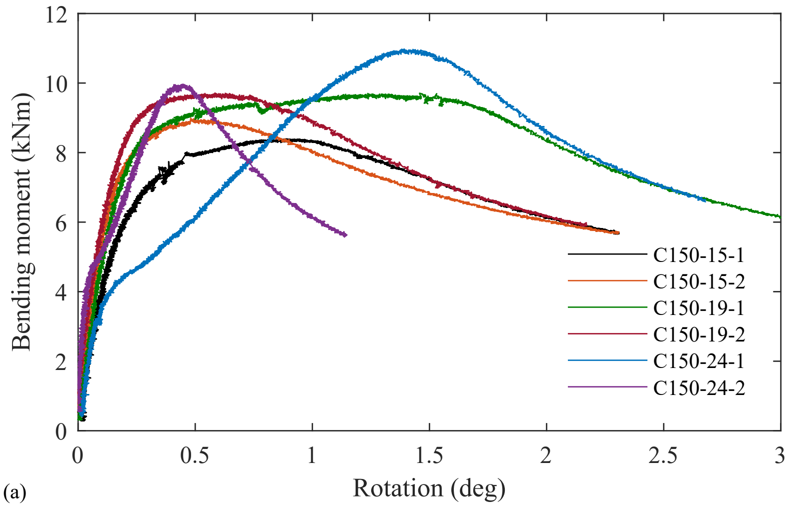

(a)

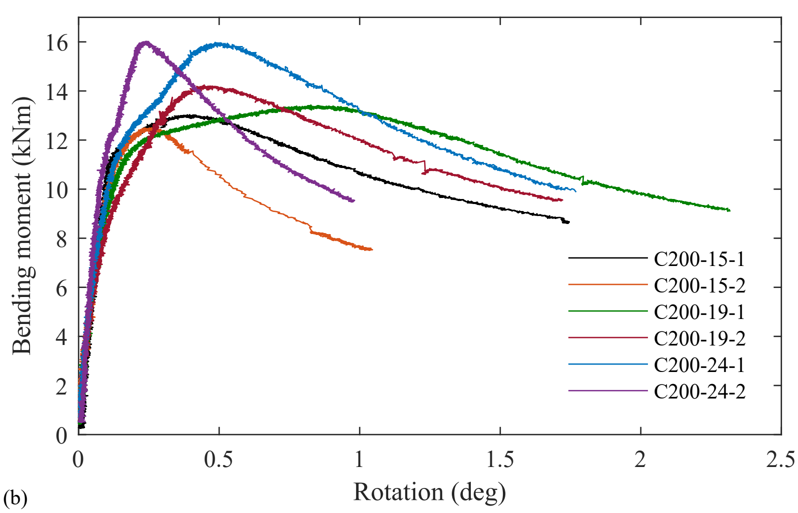

(b)

Figure 7: Moment vs. rotation curves of the tested specimens at the apex bolt-group centers (a) C150 specimens and (b) C200 specimens

Table 2: Results of the apex connections tests including initial connection stiffness and ultimate bending moment

Test	$K_{initial}$ (kNm/deg)	M_u (kNm)	$M_u/M_{y,bracket}$	$M_u/M_{y,rafter}$
C150-15-1	29.0	8.39	0.44	0.39
C150-15-2	32.3	8.99	0.47	0.42
C150-19-1	39.0	9.71	0.51	0.36
C150-19-2	36.2	9.71	0.51	0.36
C150-24-1	35.2	11.0	0.57	0.32
C150-24-2	42.5	9.97	0.52	0.29
C200-15-1	77.4	13.1	0.34	0.37
C200-15-2	86.9	12.5	0.32	0.35
C200-19-1	87.1	13.4	0.35	0.30
C200-19-2	85.4	14.2	0.37	0.32
C200-24-1	88.3	16.0	0.41	0.28
C200-24-2	95.1	16.0	0.41	0.28

respectively. The ratio of the ultimate bending moment in each test to the yield moment of the apex bracket or rafter section in each test is given in Table 2. The ultimate bending moment in the apex connections were well below the yield moment of the brackets and rafters.

5 Discussion

The average initial in-plane rotational stiffness of each apex connection size is given in Table 3. The stiffness calculated from the data shown in Figure 7 is per side of the apex connection (left and right) and is shown in Figure 8(a). These act as springs in series in the apex connection, and therefore a single equivalent spring stiffness can be calculated as given in Equation 1 and is shown in Table 3. This value can be used as a linear spring at the apex nodal location in finite element software, as shown in Figure 8(b).

$$\frac{1}{k_{eq}} = \frac{1}{k_{conn}} + \frac{1}{k_{conn}} \tag{1}$$

From Yu et al. (2005), the four main causes of rotation in a connection were the following: bolt hole elongation due to bearing of bolts on bolt-holes, slippage between plates and washers, clearances between bolts and bolt-holes allowing

Table 3: Average initial connection stiffness and ultimate bending moment for each connection pair

Connection	$K_{initial,average}$ (kNm/deg)		$M_{u,average}$ (kNm)	$\frac{I_{x,bracket}}{I_{x,rafter}}$
	per side	single spring		
C150-15	30.6	15.3	8.69	1.25
C150-19	37.6	18.8	9.71	1.00
C150-24	38.8	19.4	10.5	0.79
Average C150	35.7	17.8	-	-
C200-15	82.1	41.1	12.8	1.39
C200-19	86.2	43.1	13.8	1.09
C200-24	91.7	45.8	16.0	0.86
Average C200	86.7	43.3	-	-

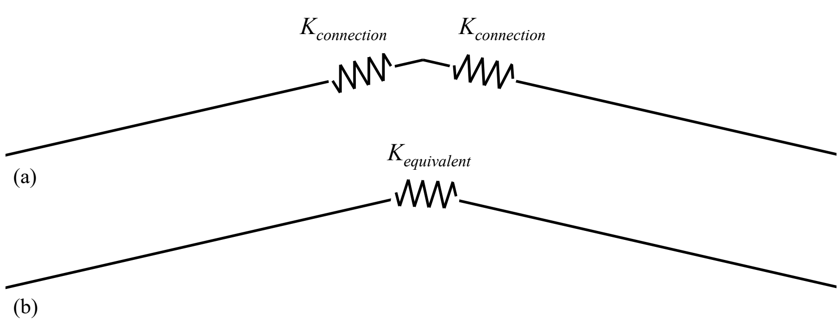

Figure 8: Apex connection in-plane stiffness springs (a) per side of connection and (b) equivalent single spring

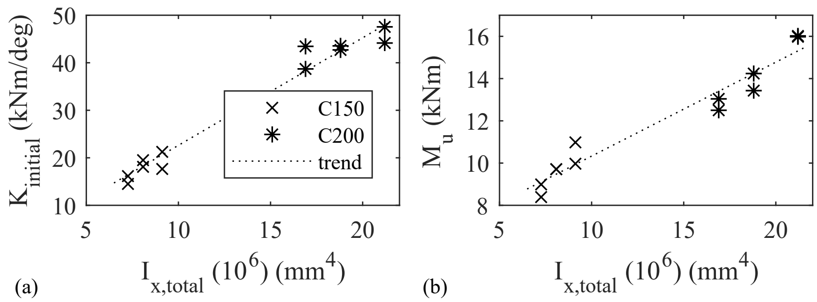

Figure 9: Relationship between $I_{x,total}$ and (a) $K_{initial}$ and (b) M_u

movement, and flexural and shear deformation of brackets and rafter members. The absence of bolt-hole elongation indicates that rotation in the connections was not a result of bearing of bolts on bolt-holes. Additionally, there was no indication of bolt-slippage in the experiments. All bolts were tightened using the same method. For apex connections of a specified rafter depth (C200 or C150), the only changes to the connections was channel thickness, therefore flexural and shear deformation of the brackets and rafters is the remaining factor which could cause variation in the rotation of the connection, for a given connection depth.

Increasing the channel section thickness from 1.5mm to 2.4 mm resulted in an 12% and 27% increase in initial moment-rotational stiffness for C200 and C150 sections, respectively. For each group of tests (C150 or C200), an increase of rafter thickness increases the second moment of area, I_x, of the rafter, and hence increases $I_{x,total}$ of the connection ($I_{x,total} = I_{x,bracket} + I_{x,rafter}$). It is shown in Table 3 that as the rafter thickness increases, there is a higher ultimate moment capacity of the connection, despite failure being governed by buckling of the brackets. This is due to the thicker rafter sections having a higher second moment of area, and hence providing greater restraint to the compression edge of the apex brackets, thereby increasing the bracket buckling capacity. Figure 9 plots the initial in-plane connection stiffness vs. $I_{x,total}$ and the ultimate bending moment of the connection vs. $I_{x,total}$. There is an approximate linear trend between both the initial in-plane connection stiffness and the ultimate bending moment with the total second moment of area of the apex connection. It is therefore hypothesized that the combined second moment of area is the major factor affecting the initial connection stiffness and ultimate bending moment capacity, for similar connection designs.

Overall the C200 connections have a higher $K_{initial}$ and greater M_u than the C150 connections. As a result of the larger channel sections and brackets in the C200 connections, $I_{x,total}$ is greater, and additionally the bolt-group area in the apex bracket is larger and has more bolts, than in the C150 connections. Changes in apex bracket size and bolt configurations (bolt-group size) have been found to have a significant impact on the moment-rotational stiffness of connections (Lim and Nethercot, 2003; Zhang et al., 2016).

As the thickness of the connected rafters increases, the initial in-plane rotational stiffness increases. However, this initial linear region is significantly smaller for C150-24 specimens. In Figure 10(b) it is shown that the C150-24 curves are almost bi-linear, whereas the C150-15 and C150-19 specimens (Figure 10(a)) do not show this behavior. In Table 3, the ratio of $\frac{I_{x,bracket}}{I_{x,rafter}}$ is presented. The lowest ratio is 0.79 for the C150-24 specimens. In this case the rafter sections are significantly flexurally stiffer than the apex brackets, and this creates a local weak area in the apex connection. It is hypothesized that as loading increases, it becomes easier for the apex bracket to deflect rather than bending in the rafters or in the combined system, which results in an earlier loss of stiffness in the connection compared to the specimens with higher $\frac{I_{x,bracket}}{I_{x,rafter}}$ ratios. It could be argued that the C200-24 specimens (Figure 10(d)) slightly show a similar trend to the C150-24 specimens, although the change in slope is much less pronounced and occurs at a higher bending moment. The threshold ratio of $\frac{I_{x,bracket}}{I_{x,rafter}}$ which causes the moment-rotation behavior to change from having a long initial linear region to a shorter region should be investigated, as an early loss of stiffness in the connection would be undesirable.

6 Conclusions

An experimental program was carried out on a series of twelve apex connections of portal frames composed of back-to-back lipped channels for the rafters and back-to-back lipped L-plates for the apex brackets. The rafters had a depth of either 200 or 150 millimeters, and thickness of 1.5, 1.9, or 2.4 millimeters. The apex brackets were 2.4 millimeters thick, and the dimensions varied to match with the connecting channel sections. The channels and brackets were connected together with bolts through the webs of all members. The average initial in-plane rotational stiffness was determined to be 17.8 kNm/deg and 43.3 kNm/deg for C150 and C200 connections, respectively, for a single apex spring. Failure of all specimens resulted from buckling of the apex bracket web. It was found that the initial in-plane rotational stiffness and the ultimate moment of the apex connection were proportional to the second moment of area of the connection ($I_{x,total}$ = $I_{x,bracket}$

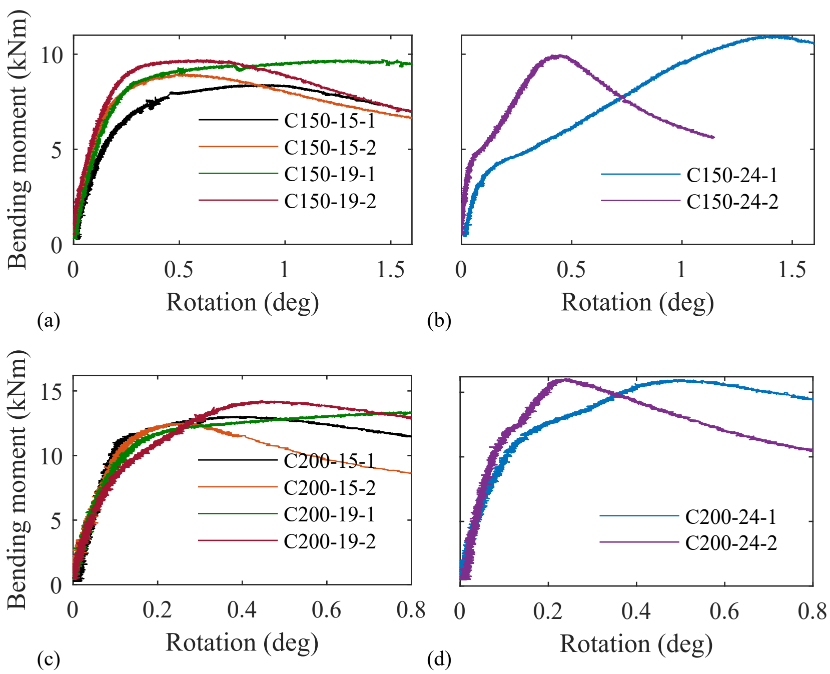

Figure 10: Moment vs. rotation curves (a) C150-15 and C150-19, (b) C150-24, (c) C200-15 and C200-19, and (d) C200-24 specimens

+ $I_{x,rafter}$). However, the range of the initial linear stiffness region was affected by the ratio of $\frac{I_{x,bracket}}{I_{x,rafter}}$, where specimens with a low $I_{x,bracket}$ relative to $I_{x,rafter}$ resulted in an early reduction of apex connection stiffness. Therefore, if higher connection stiffness is desired, the thickness of the connected elements should be considered when designing apex connections.

7 Acknowledgments

This research was supported by the Australian Research Council under Linkage Grant LP120200528. The tests were performed in the J.W. Roderick Structures Laboratory at the University of Sydney. The authors would like to thank BlueScope Lysaght for providing testing materials.

References

AS 1391 (2007). *Australian Standards 1391: Metallic Materials - Tensile Testing at Ambient Temperature*.

Bendit, J. (2017). “Experimental Investigation of Apex Connection Moment-Rotational Stiffness in Cold-Formed Steel Portal Frames”. Undergraduate Honors Thesis. Undergraduate Honors Thesis, The University of Sydney.

Dubina, D., A. Stratan, A. Ciutina, L. Fulop, and Z. Nagy (2004). “Performance of ridge and eaves joints in cold-formed steel portal frames”. *Proceedings Seventeenth International Specialty Conference on Cold-Formed Steel Structures*. Orlando, Florida, pp. 727–741.

Kirk, P. (1986). “Design of a cold formed section portal frame building system”. *Proceedings Eighth International Specialty Conference on Cold-Formed Steel Structures*. St. Louis, Missouri, pp. 295–310.

Lim, J. and D. Nethercot (2003). “Ultimate strength of bolted moment-connections between cold-formed steel members”. *Thin-Walled Structures* 41, pp. 1019–1039.

Lim, J. and D. Nethercot (2004). “Stiffness prediction for bolted moment- connections between cold-formed steel members”. *Journal of Constuctional Steel Research* 60, pp. 85–107.

Peng, J. (2017). “Experimental Investigation of Apex Connection Stiffness in Cold-Formed Steel Portal Frames”. Undergraduate Honours Thesis. Undergraduate Honors Thesis, The University of Sydney.

Yu, W., K. Chung, and M. Wong (2005). “Analysis of bolted moment connections in cold-formed steel beamcolumn sub-frames”. *Journal of Constructional Steel Research* 61.9, pp. 1332–1352.

Zhang, X., K. J. Rasmussen, and H. Zhang (2016). “Experimental investigation of locally and distortionally buckled portal frames”. *Journal of Constructional Steel Research* 122, pp. 571–583.